ST. ANTHONY FALLS LABORATORY
Engineering, Environmental and Geophysical Fluid Dynamics

Project Report No. 499

A Model for Mitigation of Surface Runoff Temperatures by a Wetland Basin and a Wetland Complex

by

William Herb, Omid Mohseni, and Heinz Stefan

Prepared for the
Vermillion River Watershed Joint Powers Organization, Dakota County, Minnesota

with previous support from
Minnesota Pollution Control Agency
St. Paul, Minnesota

July 2007
Minneapolis, Minnesota

Abstract

This report describes hydro-thermal models developed to simulate temperature mitigation of surface runoff for wetland basins. Two models are described: 1) a dead zone model, which is a modification of the previously developed vegetated pond model to include flow short circuiting and 2) a new, multi-cell model that attempts to model lateral temperature gradients between a short-circuiting channel and a wetland basin. Both models predict that a well-vegetated wetland basin can provide substantial thermal mitigation. The dead zone model is used in conjunction with a model for a wet pond to simulate the response of a wetland complex to stormwater inflow for 6 years of observed storm events. The wetland complex was found to reduce runoff temperature by 2.6 °C, on average for Minnesota climate conditions, compared to unmitigated runoff from an asphalt parking lot. The wetland complex did not, however, reduce the average runoff temperature for all storms. During very warm weather following storm events, the wetland outflow temperature did exceed 20 °C for periods of up to several days.

Table of Contents

I. Introduction

Residential and commercial development dramatically alters a drainage system by landscaping, including changes in topography, surface cover (pavements and buildings), and addition of new storm sewers and detention ponds. This produces short-term (single rainfall event) effects on stream temperatures, and long term (base flow) effects through changes in infiltration and ground water flow. The degradation of trout habitat by these short and long-term thermal effects is a particular concern of state agencies such as the Minnesota Pollution Control Agency and the Minnesota Department of Natural Resources. A current research project at SAFL is to develop a simulation tool to enable prediction of the effects of residential and commercial developments on the temperature of nearby streams. A key component of this tool is a hydro-thermal model to simulate the temperature and flow rate of stormwater runoff. Models have been developed that give continuous or event-based temperature and flow simulations for a variety of land uses, including pavement and vegetated land surfaces (Herb et al. 2006b).

This report describes the addition of hydro-thermal models for wetland basins. Two models are described: 1) a dead zone model, a modification of the previously developed vegetated pond model to include flow short circuiting and 2) a new, multi-cell model that attempts to model lateral temperature gradients between a short-circuiting channel and a wetland basin. Both models predict that a well-vegetated wetland basin can provide substantial thermal mitigation. The dead zone model is used in conjunction with a model for a wet pond to simulate the response of a wetland complex to stormwater inflow for 6 years of observed storm events.

II. Dead zone model for a wetland basin

One approach to model a wetland basin is to divide the basin into a dead zone, i.e. a region of the basin with relatively low flow, and a channelized region that has lower flow resistance and therefore faster flow (Figure 1).

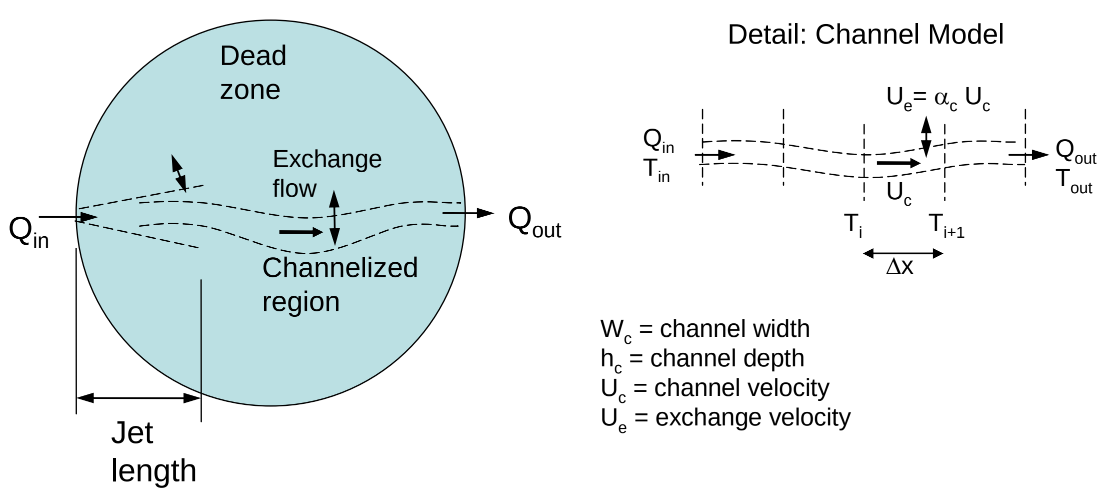

Figure 2.1. Schematic representation of a wetland with a dead zone region and a channelized region.

Dead zone models for wetlands have been used in the past to estimate the thermal impact of wetlands on surface flows (Andradottir and Nepf 2000). The dead zone model used in this study is similar to the model created by Andradottir and Nepf, but includes consideration of jet entrainment at the inflow and consideration of unsteady hydrologic conditions.

II.1 Model for the dead zone

The vegetated pond model (Herb et al. 2006b) is suitable for modeling the dead zone. For periods of zero or very small inflow, the dead zone model works in exactly the same way as the vegetated pond model; it includes consideration of atmospheric heat transfer in the presence of emergent vegetation, heat transfer to the sediment, and wind-mixing/stratification processes. Outflow rate is calculated based on the basin water elevation in relation to a specified outlet structure, and outlet temperature is calculated based on the vertical profile of temperature in the basin. A model for the effect of emergent vegetation on surface heat transfer processes is included in the dead zone model. The vegetation model considers absorption of solar and long wave radiation by the plant canopy and re-radiation to the water surface, based on an estimated plant canopy temperature. The vegetation model is described in more detail in SAFL Project report 478 (Herb et al. 2006c)

II.2 Model for the channelized area

During inflow events, a channel model is activated that considers a flow velocity and water temperature along a channelized region that is different from those in the dead zone region. At the inflow point, an integral jet model is used to estimate the jet length and the volume of entrainment of ambient water into the inflow jet (Appendix I). For the remaining distance to the outlet, a 1-D channel model is used to calculate the water temperature including advection and exchange flow with the dead zone (Figure 2.1). The channel flow rate is assumed to be equal to the outflow rate at the outlet structure, and constant over each time step. Over the length of each sub-division of the channel, a heat balance is used to calculate the change in temperature:

(2.1) $$\frac{\partial T}{\partial t} = U_c \frac{\partial T}{\partial x} + 2U_e \frac{\partial T}{\partial y}$$

where T is the channel temperature, x is streamwise distance, y is lateral (width) distance, U_c is the channel velocity, and U_e is the exchange flow velocity. A discretized form of equation (2.1) is used in the finite-difference model:

(2.2) $$T_{i+1}^{j+1} = \frac{T_{i+1}^{j} + U_c T_i^{j+1} \frac{\Delta t}{\Delta x} + 2U_e \frac{\Delta t}{w} T_b^j}{1 + U_c \frac{\Delta t}{\Delta x} + 2U_e \frac{\Delta t}{w}}$$

where T_b is the basin temperature (dead zone temperature), Δx is the length of the descritized channel volume, Δt is the analysis time step, and w is the channel width. Atmospheric heat exchange is not included in the channel model, because atmospheric heat transfer in the dead zone region, and subsequent exchange flow with the channel, are considered more significant processes. Multiplication of the exchange flow velocity (U_e) by 2 takes into account that exchange flow takes place on both sides of the channel, i.e. exchange with two dead zones at the same temperature.

II.3 Exchange Flow

Exchange flow between the channelized region and the basin can be driven by temperature differences, wind, and the mean channel flow. Exchange flow due to a mean flow in the channel has been addressed for channelized wetlands and for inflow jets in lakes (Fang and Stefan, 1991, 2000; Andradottir and Nepf, 2000). The crucial parameter to be determined is the exchange coefficient, α, the ratio of the mean flow velocity to the lateral exchange flow velocity.

An estimate of the exchange flow rate driven by the temperature differences between the channel and the dead zone region was derived from the potential energy (E_p) available for mixing from a temperature difference between two basins of depth h and width w:

(2.3) $$E_p = \frac{\Delta\rho\, g\, w\, h^2}{2}$$

where $\Delta\rho$ is the difference in density due to the temperature difference, and g is the acceleration of gravity. This potential energy (per unit length along the channel) is used to create a buoyancy driven exchange flow between the channel and the dead zone. More specifically potential energy (E_p) is used to (1) create kinetic energy (E_k), i.e. accelerate stagnant water to some velocity and (2) balance friction loss (E_f).

(2.4) $$E_k = \rho \frac{V^2\, w\, h}{2}$$

(2.5) $$E_f = \rho\, \hat{a}\, C_D V^3 \Delta t\, w\, h$$

where V is the exchange flow velocity, $\hat{a}$ is the plant surface area per unit volume, and C_D is the drag coefficient of the plants. Using data from Hall and Freeman, a full density plant canopy (800 stems per square meter) is assigned $\hat{a} = 7.0\ m^2$ surface area per m^3 volume. For relatively dense wetland vegetation, it was found that the friction loss term greatly exceeded the kinetic energy term, allowing the potential energy to be equated to the friction energy loss. This leads to equation (2.6) as an estimate for the exchange flow velocity:

(2.6) $$V = \left(\frac{1}{\rho} \frac{\Delta\rho}{\Delta t} \frac{g\, h}{2\, \hat{a}\, C_D} \right)$$

During simulations, this exchange flow estimation resulted in an exchange flow velocity on the order of several mm/sec. The distance traveled at this velocity over the time step (30 min) results in a distance on the order of 3 meters, or the same order as the channel width. This indicates that buoyancy driven exchange flows driven by water temperature differences are quite important.

III. Multi-cell model for a wetland basin

III.1 Flow model

The dead zone model treats the non-channelized area, i.e. the dead zone region as a single, well mixed volume with a uniform temperature. Uniform temperature is assured only by mixing of the dead zone water. However, mixing in a wetland basin is inhibited by submersed and emergent vegetation, and therefore some temperature gradient between the channel and the dead zone is expected.

During inflow events, substantial flow must occur to all portions of a wetland basin to raise the basin water level. To estimate this flow, the wetland basin was divided into sub-basins as shown in Figure 3.1. For each time step, an overall water balance for the basin was used to determine the change in water level (Δh).

$$(3.1) \qquad \Delta h = \frac{(Q_{in} - Q_{out})\Delta t}{A_s}$$

where t is time, Δt is the time step, Q_{in} and Q_{out} are the inflow and outflow rates for the wetland, and A_s is the total surface area of the basin. Q_{in} is specified, while Q_{out} is determined based on the outlet structure for the basin and the current basin depth.

For each sub-basin, a volume balance for each time step gives equations of the following form:

$$(3.2) \qquad \frac{As_{i,1}\Delta h}{\Delta t} = Q_{i-1,c} - Q_{i,c} - Q_{i-1,bc}$$

The flow rates Q in equation (3.2) are defined in Figure 3.1; the subscripts c and b denote channel and basin, respectively. For a ten-cell model, writing a volume balance equation for each cell, including the specified inflows and outflows, results in 9 independent equations with 12 unknowns. Additional equations for the flow components may be found by considering the flow resistances of the various cells, based on their geometry and vegetation density. For the present study, an overall split in flow between the channelized area and the remainder of the wetland basin is assumed, based on the overall flow resistance along the two flow paths (Figure 3.2). An expression (equation 3.3) for the relative flow resistance of the channel and the remainder of the basin as shown in Figure 3.2 was derived from Manning's equation.

$$\frac{R_b}{R_c} = \left(\frac{h_b}{h_c}\right)^{2/3} \left(\frac{Ac_b}{Ac_c}\right)\left(\frac{n_c}{n_b}\right) \quad (3.3)$$

where Ac is the average cross-sectional area and n is Manning's roughness coefficient, and the subscripts c and b denote channel and basin, respectively. n is estimated from the specified vegetation density for the basin and the channel, using relationships given by Hall and Freeman (1994). Equation 3.4 is used to specify the flow ratios for the intermediate cells (e.g. i=2, 3, 4 in Figure 3.1) to obtain a solution.

$$\frac{Q_{i,b}}{Q_{i,c}} = \frac{R_c}{R_b} \quad (3.4)$$

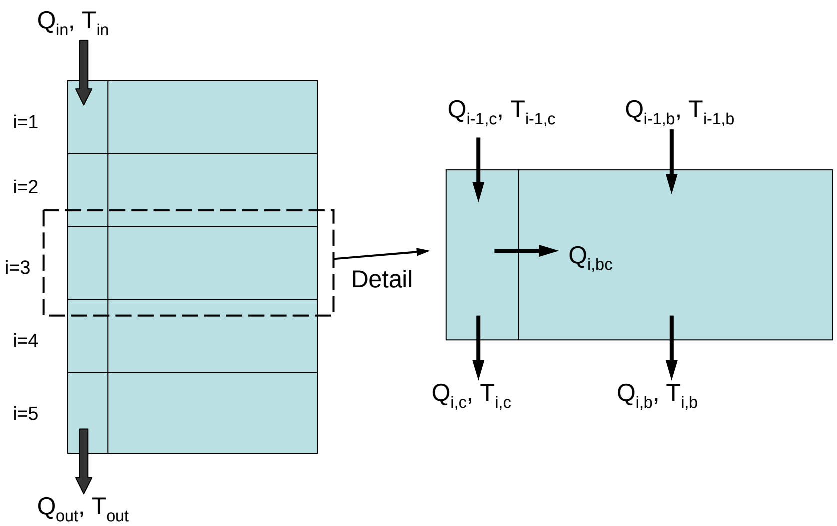

Figure 3.1. Schematic diagram for the multi-cell model.

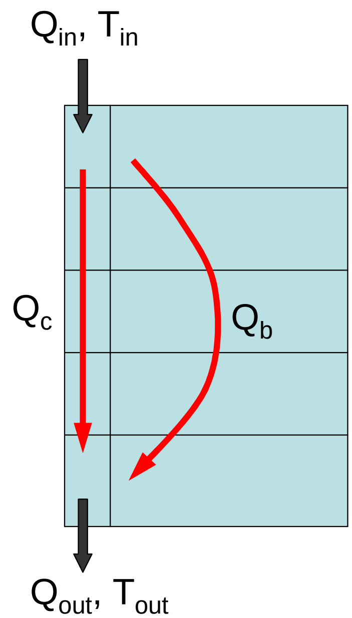

Figure 3.2. Diagram of flow partitioning between the channelized area and the remainder of the basin.

III.2 Temperature model

The water temperature in each cell is determined for each time step based on inflows and outflows, atmospheric heat exchange, and heat conduction to the sediment. With the notation used in Figure 3.1 for flow rates Q and water temperatures T, the heat balance for each cell may be written as

$$(3.5)\quad \frac{\Delta(V_{i,c}T_{i,c})}{\Delta t} = Q_{i-1,c}T_{i-1,c} - Q_{i,c}T_{i,c} - Q_{i,bc}T_{i,c} + \frac{(Ha+Hs)As_{i,c}}{\rho C_p}$$

where V is the cell volume, Ha and Hs are the atmospheric and sediment heat flux, respectively, and ρ C_p is the product of density and specific heat for water. The atmospheric heat flux is calculated for each cell using the formulation for vegetated ponds (Herb et al. 2006b, 2006c). Atmospheric heat flux terms include incoming solar radiation, incoming long wave radiation, back radiation, convection, and evaporation. The effect of emergent vegetation is important to include because it reduces solar radiation input to the water (Herb et al. 2006b). The sediment heat flux is calculated for each cell based on a multi-layer heat conduction model, similar to the heat conduction model used in stormwater pond and vegetated pond models (Herb et al. 2006a, 2006b).

IV. Simulation Results

IV.1 Response of the dead zone model and cell model to inflow test cases

The models were set up to approximate the basin geometry of basin WC-9 at the Shakopee wetland previously used as a test case for the vegetated pond model (Herb et al. 2006b). Based on a previous model calibration (Herb et al. 2006b), the vegetation density in the wetland basin was set to 0.7 (70% cover). To test the response of the models, inflow scenarios of 2 hr and 24 hr duration and inflow volumes of 500 m^3 and 4000 m^3 were created (Table 4.1), and used as model inputs. The two hour duration events are intended to simulate the response of the wetland to direct runoff from an impervious watershed, while the 24 hour duration events are intended to simulate the response to flow from a wet detention pond upstream of the wetland. In the latter case the flow is of longer duration and at a lower rate compared to the former. An inflow volume of 500 m^3 is much less than the stored basin volume, while an inflow volume of 4000 m^3 is of the same order as the wetland basin volume. In all cases, the model was run to simulate 10 days, using climate data from the Shakopee wetland site for the period June 21, 2006 to July 1, 2006 (Figure 4.1). The recorded climate data include a rainfall event starting at 14:00 on June 24, which was used as the specified time for all inflow events listed in Table 4.1.

Table 4.1. Summary of four test case inflow events used in model evaluation. The specified inflow rate and temperature are constant over the specified duration.

Inflow Case	Duration (hours)	Total Volume (m^3)	Inflow Rate (m^3/sec)	Inflow Temperature (^oC)
#1	24	4000	0.0463	25
#2	2	4000	0.556	25
#3	24	500	0.00579	25
#4	2	500	0.0694	25

Time series of the mean water temperature in the wetland basin simulated by the two models are given in Figure 4.2. The basin temperature is averaged over depth for the dead zone model and averaged horizontally over distance for the cells model. The cells model gives a slightly higher mean basin temperature for the given climate forcing, because it uses a well mixed water column, whereas the dead zone model includes the effect of temperature stratification on atmospheric and sediment heat transfer.

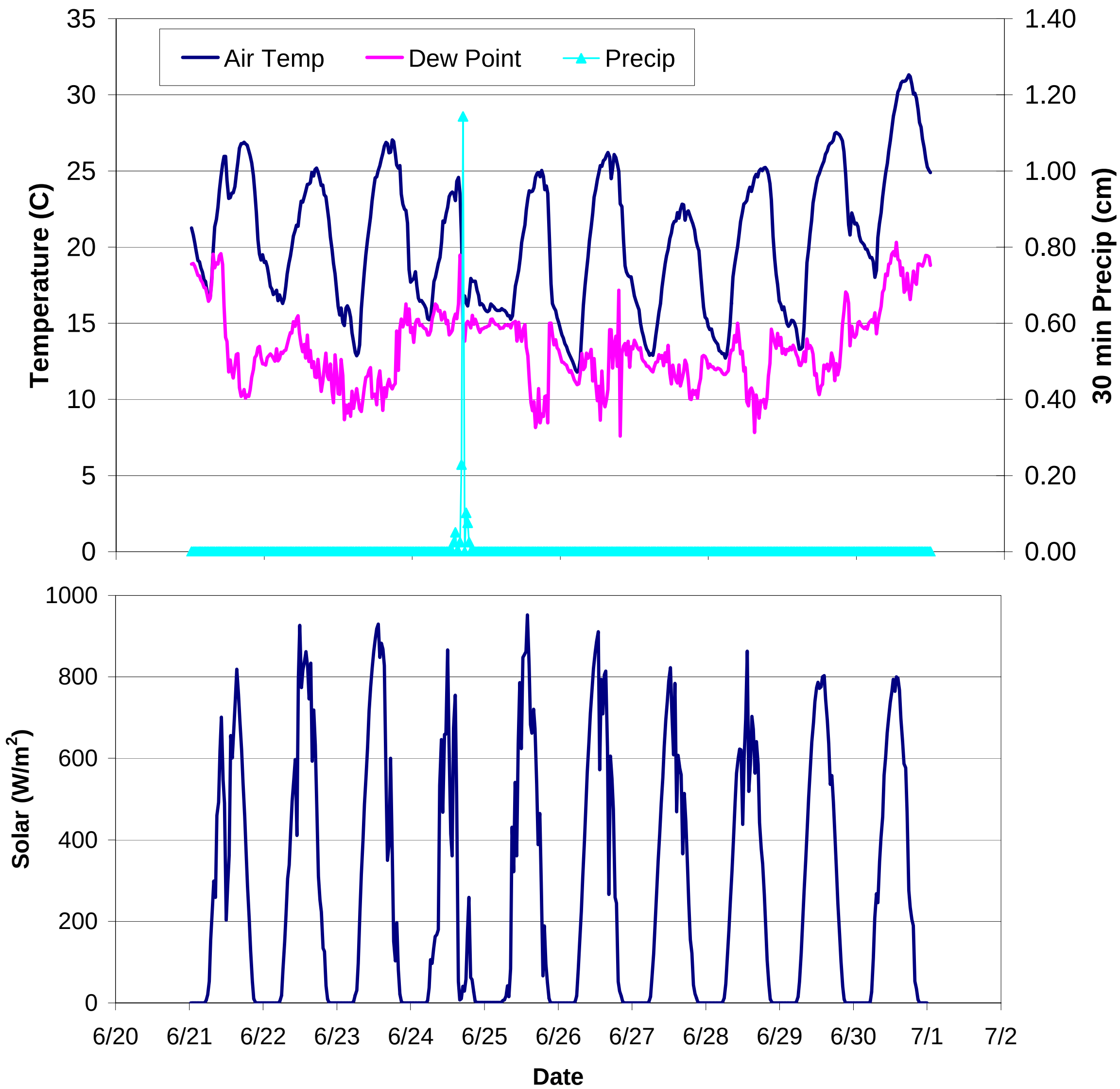

Figure 4.1. Observed climate data from the Shakopee wetland, June 21 – July 1, 2006.

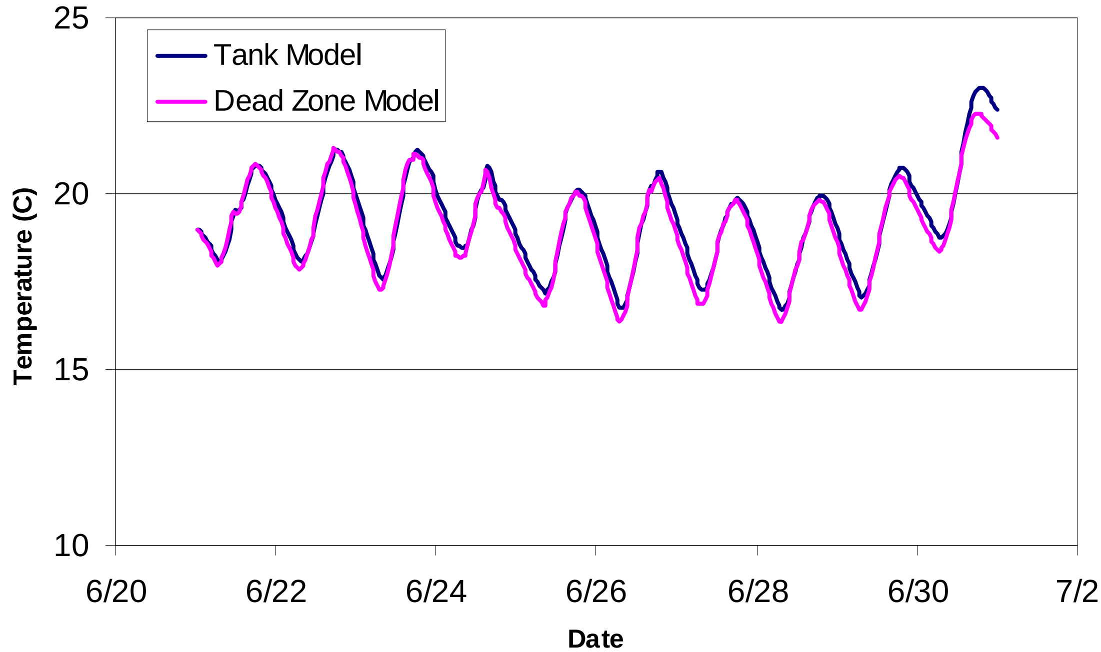

Figure 4.2. Simulated average water temperature in the wetland basin in response to the climate forcing given in Figure 4.1, with no inflows specified.

Figure 4.3 gives the response of the dead zone model to the Case 1 inflow event (Table 4.1). The outlet temperature is very close to the basin temperature, due to the relatively long wetland basin length (100 m) and the specified exchange flow coefficients. Although 25 °C water is flowing into the wetland basin for a 24 hour period, the basin temperature cools over this time period due to atmospheric and sediment heat transfer. Figure 4.4 shows the temperature gradient in the channelized area from the inlet to the outlet at the end of the Case 1 inflow event, with the basin temperature for reference. The 25 °C inflow is reduced to basin temperature via jet entrainment (the first 20 m) and exchange flow with the basin (20 – 60 m). Figure 4.5 gives the response of the dead zone model to the Case 2 inflow event. Compared to Case 1, the relatively short duration and high inflow rate lead to a large increase in basin temperature, to 22.5 °C. However, the basin cools relatively quickly after the inflow event. As a result, the average outflow temperature for Case 2 is only slightly higher (19.85 °C) than for Case 1 (19.62 °C), as summarized in Table 4.2. The total heat energy entering and exiting the wetland basin are also given in the table for each case, using a reference temperature of 20 °C.

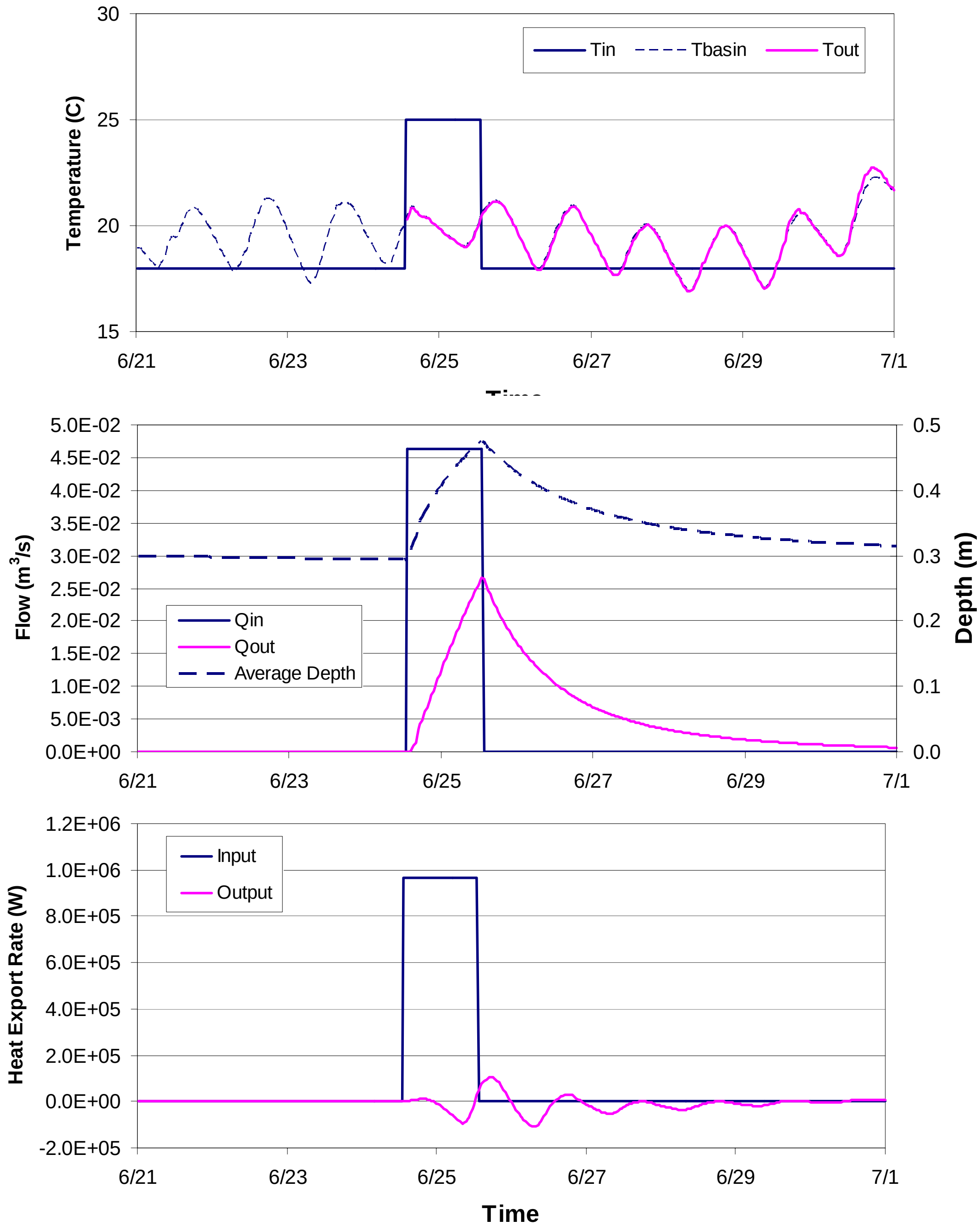

Figure 4.3. Response of the dead zone model to the Case 1 inflow event. The upper panel gives wetland basin outflow temperatures, the center panel gives water outflow rates and water depths, in the wetland basin, and the lower panel gives heat input and heat export rates for a reference temperature of 20 °C.

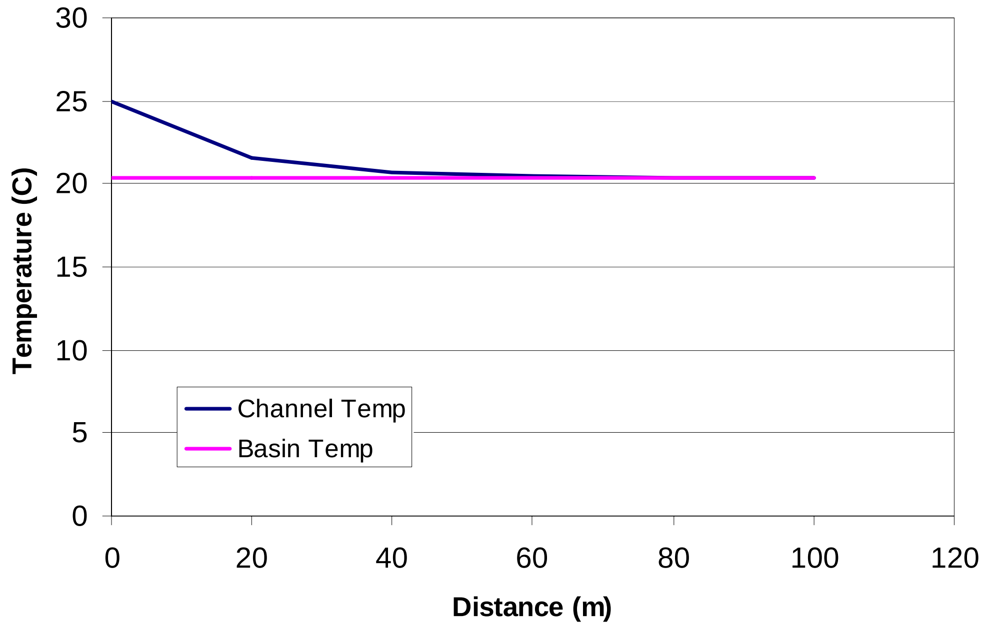

Figure 4.4. Water temperatures in the channel and the dead zone region vs. distance along the channel as simulated by the dead zone model at the end of the Case 1 inflow event.

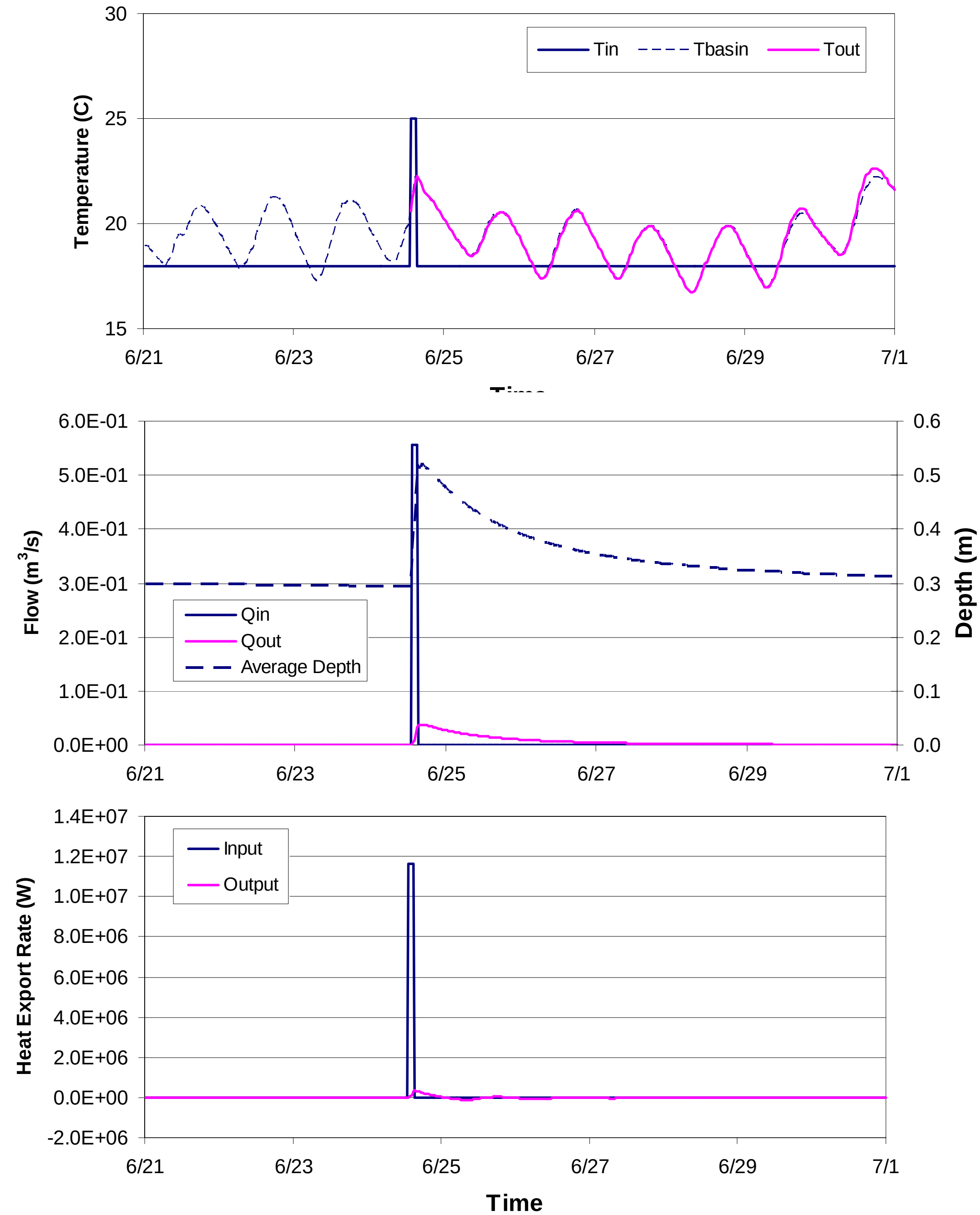

Figure 4.5. Response of the dead zone model to the Case 2 inflow event. The upper panel gives wetland basin outflow temperatures, the center panel gives water outflow rates and water depths, in the wetland basin, and the lower panel gives heat input and heat export rates for a reference temperature of 20 °C.

Figure 4.6 gives the response of cells model to the Case #1 inflow event. The outlet temperature is lower than the average basin temperature during the inflow event, due an upstream-downstream temperature gradient in the basin (Figure 4.7). For Case 1, the flow-weighted average outlet temperature for the cells model is about 0.9°C lower than that for the dead zone model. For Case 2, the average outlet temperature predicted by the cells model is 0.5°C lower than that predicted by the dead zone model.

Table 4.2 summarizes the simulation results for cases 1 - 4 for each model. The heat import (the heat energy contained in the specified inflow) and the heat export (the heat energy contained in the calculated outflow) are referenced to 20 °C. For the lower volume inflow events, the tank model gives only slightly lower average outflow temperatures, 0.07 °C and 0.06 °C, respectively, for Case 3 and 4. Note that the heat export from the wetland basin is negative for all cases, since the average outflow temperatures are lower than the reference temperature (20°C). Both models predict a substantial reduction in heat energy going through the wetland basin for all four inflow event cases.

Table 4.2. Summary of dead zone model and cells-model responses to inflow test events.

Dead zone model

Case	Outlet temperature, average (C)	Outlet temperature, maximum (C)	Total Heat Import (J)	Total Heat Export (J)
01	19.62	22.72	4.18E+10	-2.95E+09
02	19.85	22.65	4.18E+10	-1.24E+09
03	18.79	24.77	5.23E+09	-1.11E+09
04	18.84	24.79	5.22E+09	-1.11E+09

Cells model

Case	Outlet temperature, average (C)	Outlet temperature, maximum (C)	Total Heat Import (J)	Total Heat Export (J)
01	18.76	22.988	4.18E+10	-1.01E+10
02	19.35	23.053	4.18E+10	-5.41E+09
03	18.72	23.058	5.23E+09	-1.35E+09
04	18.78	23.068	5.22E+09	-1.33E+09

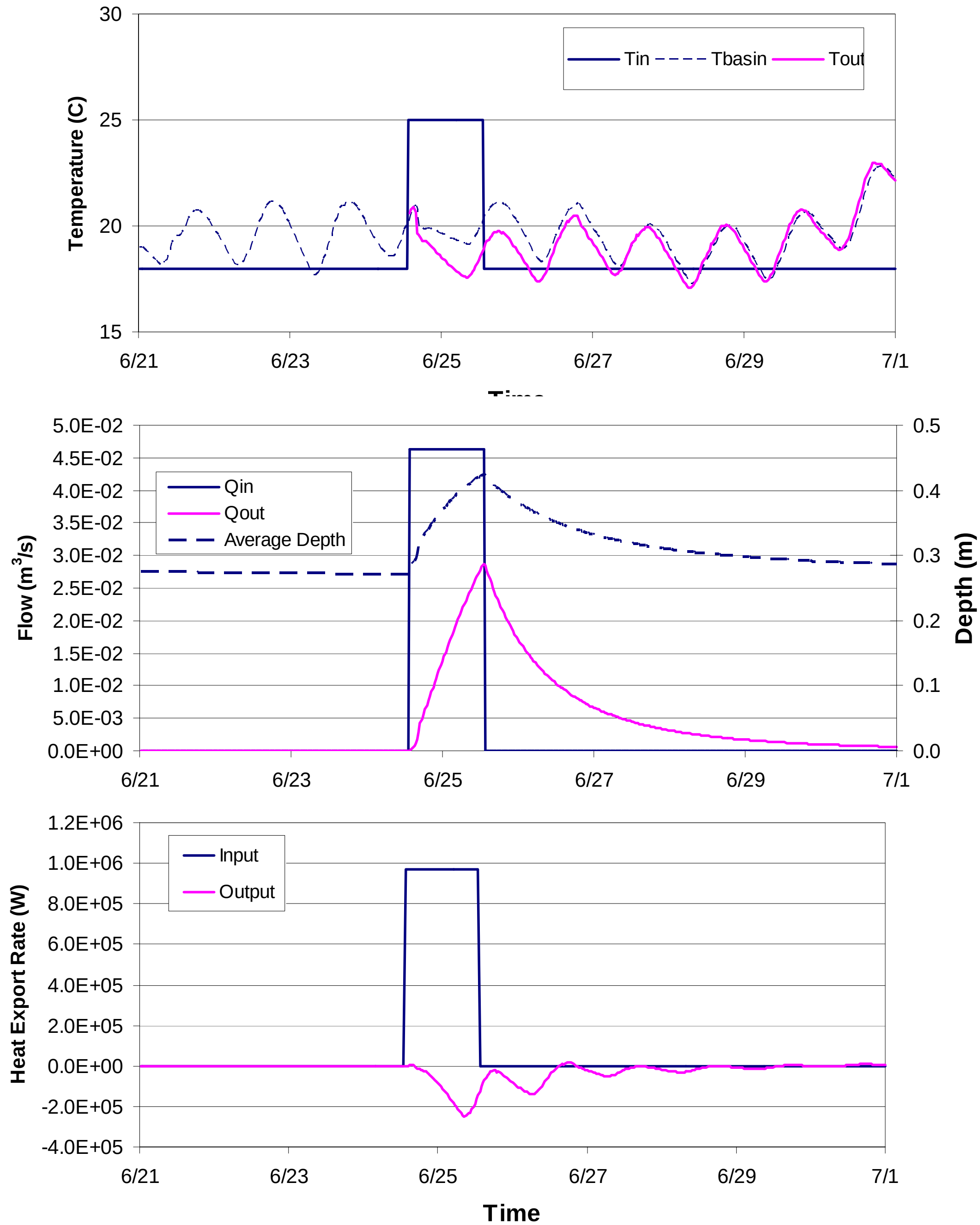

Figure 4.6. Response of cells (tank) model to the Case 1 inflow event. The upper panel gives wetland basin outflow temperatures, the center panel gives water outflow rates and water depths, in the wetland basin, and the lower panel gives heat input and heat export rates for a reference temperature of 20 °C.

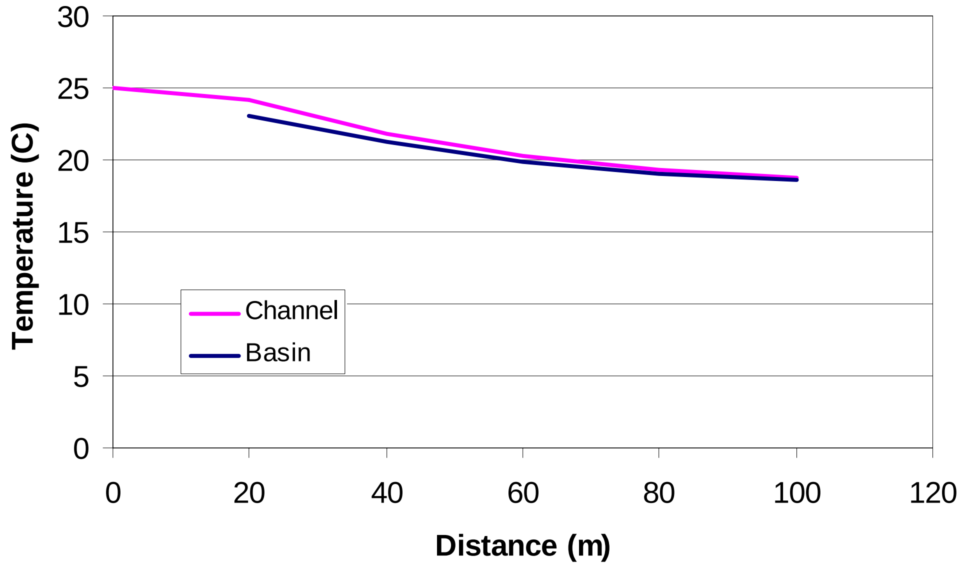

Figure 4.7. Water temperatures in the channel and the off-channel wetland basin vs. distance along the channel as simulated by the cells model at the end of the Case 1 inflow event.

IV.2 Discussion of the wetland basin model responses

For the case study wetland basin with a 100m long flow path, both models predict very little thermal short-circuiting, e.g. the temperature of the outlet flow reaches the overall basin temperature. The cells- model predicts that there may be a temperature gradient between the inflow and outflow points in both the channel and in the off-channel wetland basin, because the inflowing water is distributed throughout the basin. The longitudinal channel temperature profiles simulated by the two models are somewhat different (Figures 4.4 and 4.7). However, the outlet temperatures predicted by the two models are within 0.1 - 0.9 °C for the four inflow scenarios (Table 4.1) considered.

The average outflow temperature is a function of both the flow dynamics during the inflow event and the basin heat transfer after the inflow, since the outflow may have a much longer duration than the inflow. The cells-model may capture some of the lateral basin temperature dynamics during an inflow event, with warm inflow water tending to collect near the inlet. More detailed field data would be required to verify this simulation result, since real wetland systems are hydraulically complex compared to the geometry and flow routing assumptions used to create the models. Wind effects on flow have been ignored because emergent vegetation may dissipate wind shear.

The dead-zone model includes the effect of thermal stratification on the outlet temperature during long duration outflow events, i.e. after the inflow stops, and thus may better represent the outflow temperature dynamics after the inflow event. For this reason, the dead zone model was chosen for further work to analyze a 6 year climate data set.

V. Dead zone model sensitivity analysis

The response of the dead zone model to variations in several key input parameters was quantified using the Case 1 inflow event (24 hour duration, high volume). The model was found to be insensitive to channel width or channel length, except for very short channels. The channel length was changed without adjusting the basin volume. A 20 m long channel gave a significantly higher outflow temperature, as might be expected from Figure 4.4. A tenfold reduction in the buoyancy driven exchange flow velocity caused a small, but measurable increase (0.1 °C) in outflow temperature. In the last case, the channel length and basin volume were both reduced by a factor of 2. A reduction in basin length and volume to half the original value had a large effect on the average outflow temperature and heat export.

Table 5.1. Responses of dead zone model to variation of several channel and exchange flow parameters.

Basin Volume (m^3)	Chan. Length (m)	Chan. Width (m)	Thermal Exchange Flow Rate	Average Tout (C)	Average Tout (C)	Max. Tout (C)	Heat Export (J)
4125	100	4	nominal	19.62	19.58	22.72	-2.95E+09
4125	50	4	nominal	19.63	19.60	22.72	-2.90E+09
4125	20	4	nominal	19.90	20.60	22.57	-7.61E+08
4125	100	8	nominal	19.61	19.57	22.72	-3.04E+09
4125	100	16	nominal	19.53	19.47	22.72	-3.65E+09
4125	100	4	1/10 nominal	19.73	19.88	22.70	-2.13E+09
2063	50	4	nominal	20.57	20.54	24.85	4.18E+10

VI. Wetland basin model validation

The dead zone model described in Section II of this report is based on the vegetated pond model described in Herb et al. (2006b). The vegetated pond model was verified using climate and basin temperature data from a restored wetland complex in Prior Lake, MN, maintained by the Shakopee Mdewakanton Sioux Community Land and Natural Resources Department (Herb et al. 2006b). The channel model that was added to the vegetated pond model for this study has not been verified. 2006 data from the Prior Lake wetland did not include any major outflow events, where both significant inflow and outflow were characterized. The largest storm event in the 2006 record filled the basin to near normal depth from a relatively low level. In addition, aerial photographs and on-site inspections of the wetland basins showed open areas within the basins, but no obvious continuous channelization from the inlet to the outlet. It is therefore encouraging that the dead zone model showed minimal sensitivity to channel width (Section V).

VII. Response of a wetland complex to 6 years of storm events

Wetland mitigation systems often include one or more wet detention ponds at the upstream end, which then feed into one or more wetland basins. An example of such a system is a restored wetland complex in Prior Lake, MN, maintained by the Shakopee Mdewakanton Sioux Community Land and Natural Resources Department (Figure 7.1). For this study, a single wet pond feeding a single wetland basin was simulated (Figure 7.2). Outlet temperature and outflow rate from the wet pond were given previously by Herb et al. (2006b), using the pond model described by Herb et al. (2006a). The wet pond model was given simulated runoff from an asphalt parking lot (Figure 7.2). The simulated outflow rate and temperature were then used as the input to the wetland basin model (dead zone model). As before, the wetland basin parameters were set to mimic the WC-9 wetland basin at the Prior Lake complex, with an area of approximately 15,000 m^2 at a controlled depth of 0.3 meters. The wetland complex model was used to simulate the response to 6 years of climate data (April1- October 31). As in previous work, we used 15-minute climate data from the weather station at the MnROAD facility in Albertville, MN, obtained from the Minnesota Department of Transportation (MnDOT). Therefore, the same climate data were used to 1) simulate the runoff flow and temperature from the parking lot, 2) simulate the basin temperature and outlet flow rate and temperature of the wet pond, and 3) simulate the basin temperature and outlet flow rate and temperature of the wetland basin.

Figure 7.1. Aerial photograph of the Prior Lake wetland complex, with 2006 surface(S) and groundwater (G) temperature instrumentation sites marked.

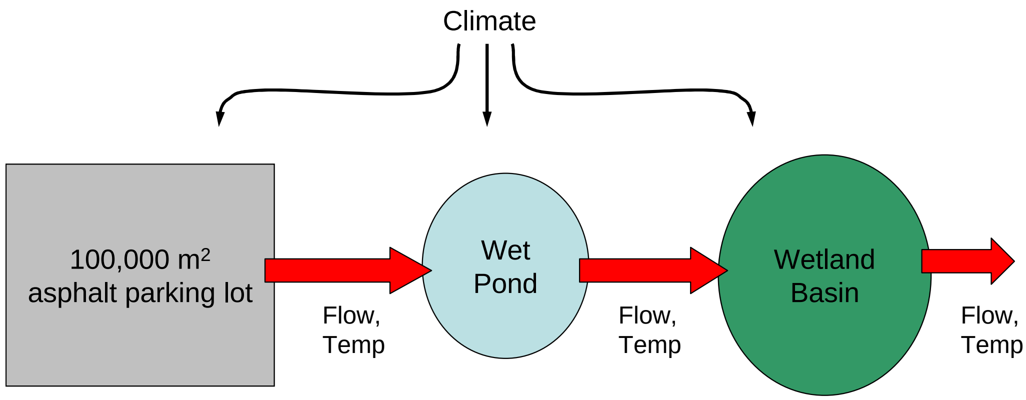

Figure 7.2. Schematic of the wetland complex system simulated in this study.

An example of wetland basin simulation results for one season (April 1 – October 31, 1998) are given in Figures 7.3 and 7.4. Simulation results for one storm event (July 30, 1999) are given in Figures 7.5 to 7.7. Outlet temperatures of the wetland basin are consistently lower than the inflow from the wet pond (Figure 7.3), although both track variations in climate after the storm event (Figure 7.5). Outlet flow rates of the wetland basin are comparable to those of the inflow (Figure 7.3), with somewhat lower peak flows during rainfall events compared to the wet detention pond (Figure 7.6). The wetland basin reduces heat export rates considerably, and the integral effect of the wetland basin over the season is substantial (Figure 7.4). The maximum heat export rate of the wetland basin is an order of magnitude lower than the peak rate for the asphalt runoff (Figure 7.7), mainly due to lower outflow rates.

The wetland complex model was run such that for each storm event, the wet pond and wetland basins had no storage capacity, so that outflow started immediately during each storm. The hydraulic response of the wetland complex was relatively long, so that drainage of 70% of the inflow volume took on the order of 3 - 4 days, as exemplified in Figure 7.5. This slow response time tends to combine the response of individual storms. To reduce storm response overlap, only storms with two days of separation from previous and subsequent storms were considered for analysis.

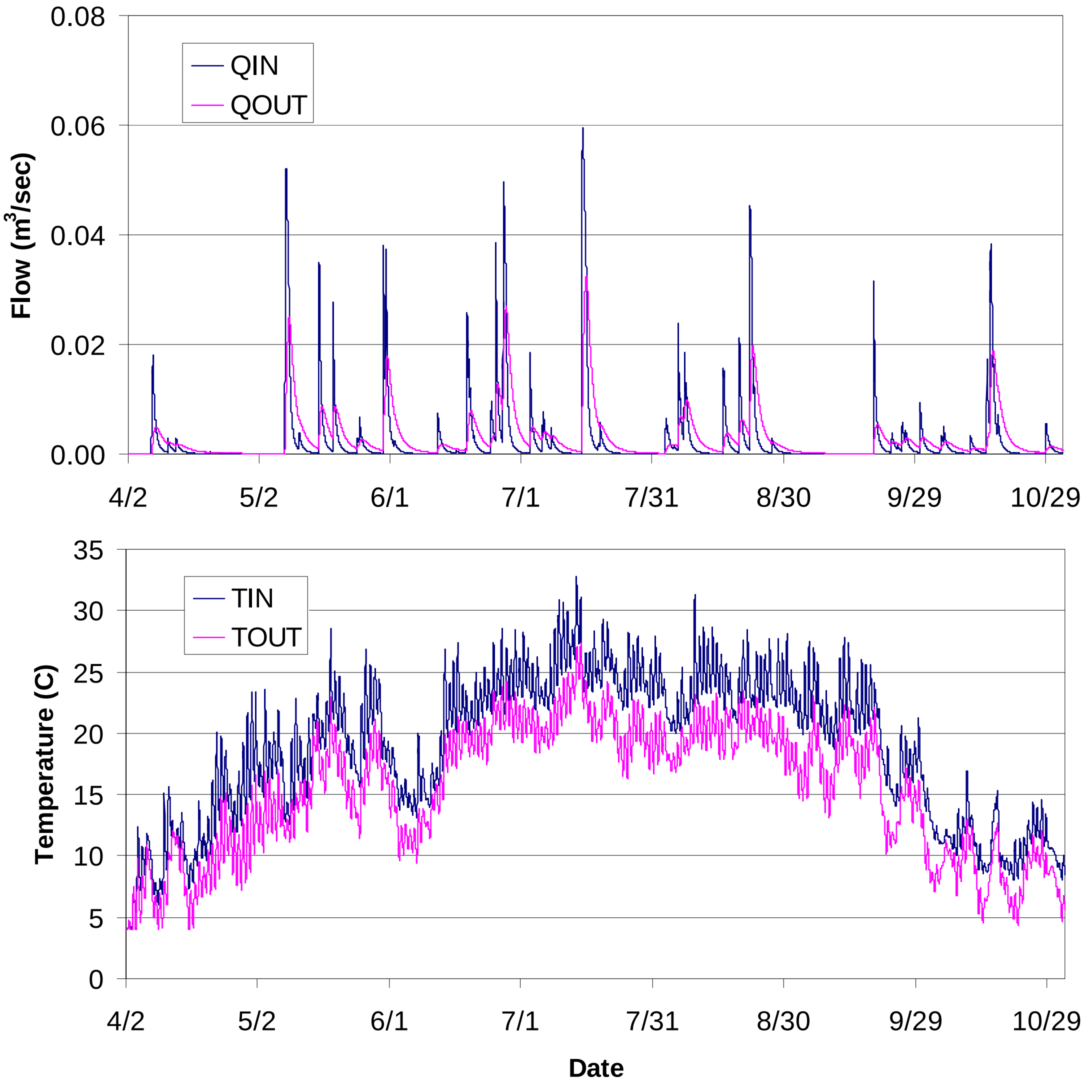

Figure 7.3. Simulated inflow and outflow rate (upper panel) and inflow and outflow water temperature for the wetland basin, April – October, 1998. Inflow is from an unshaded wet detention pond.

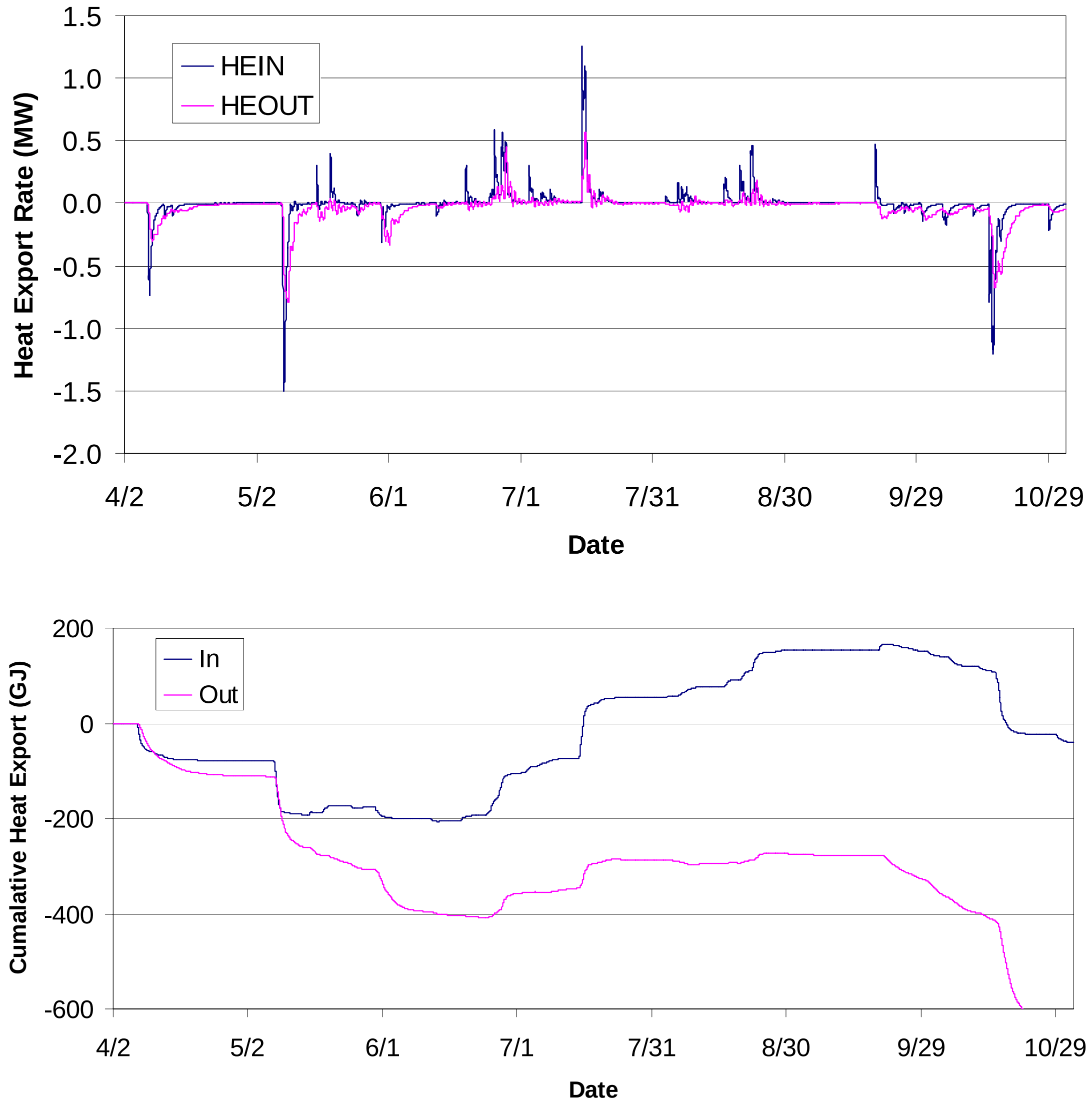

Figure 7.4. Simulated heat input and heat export rate (upper panel) and cumulative heat export (lower panel) for the wetland basin, April – October 1998. Heat export is calculated using a 20 °C reference temperature.

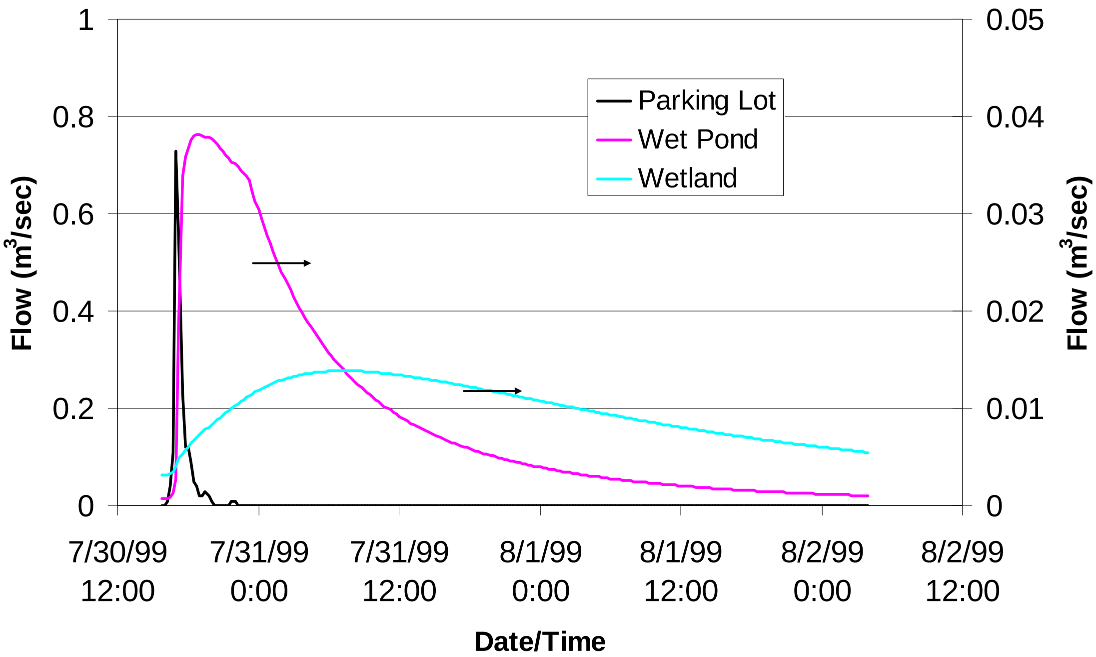

Figure 7.5. Simulated flow rate versus time for runoff from the parking lot, for outflow from the wet detention pond, and for outflow from the wetland basin. The parking lot runoff is scaled on the left, while the pond and wetland outflows are scaled on the right.

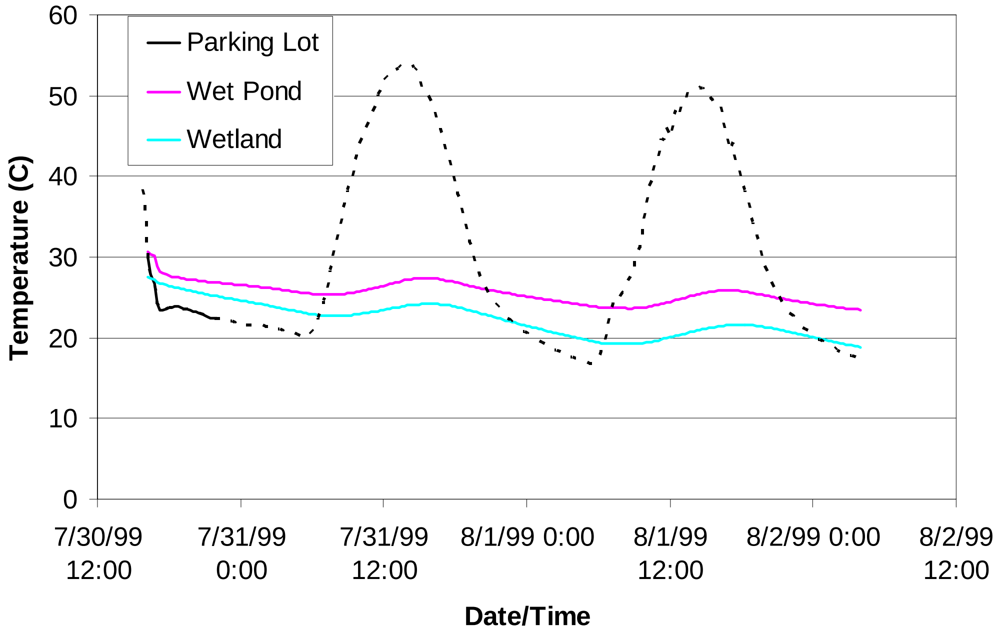

Figure 7.6. Simulated water temperature versus time for runoff from the parking lot, outflow from the wet detention pond, and outflow from the wetland basin. The parking lot runoff temperature is plotted as a solid line when flow is positive, while the dashed line gives the parking lot surface temperature with no runoff.

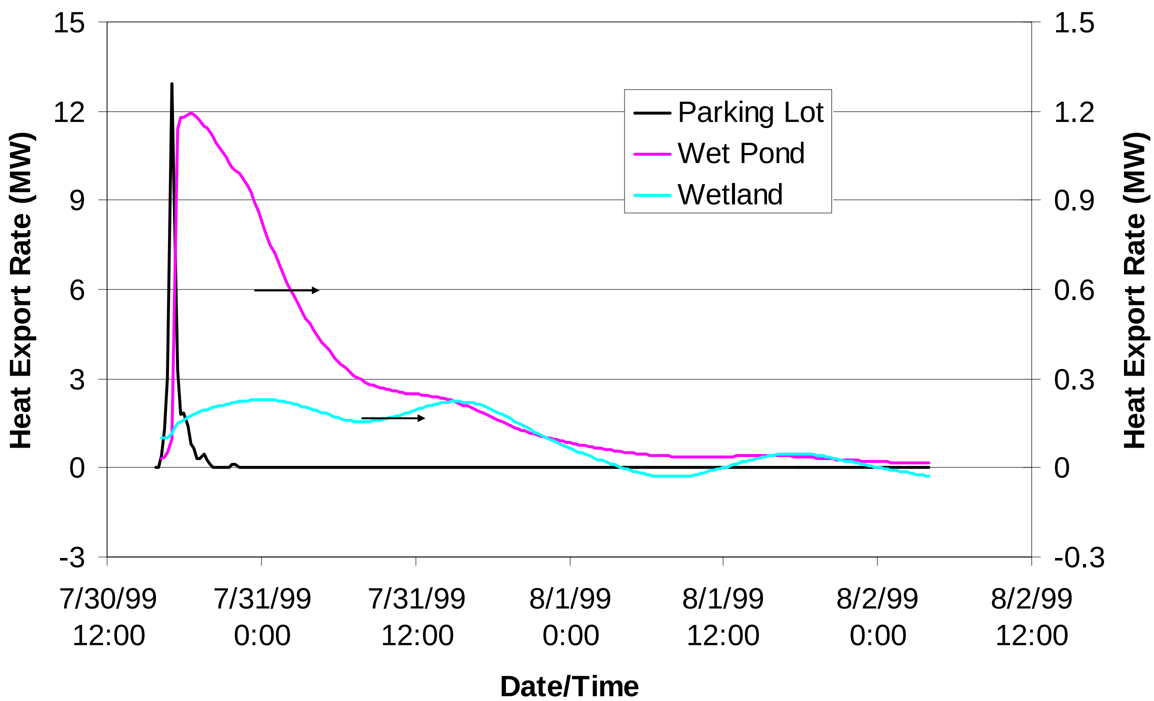

Figure 7.7. Simulated heat export rate (20°C reference temperature) vs. time of runoff from the parking lot, outflow from the wet detention pond, and outflow from the wetland basin. The parking lot is scaled on the left, while the pond and wetland are scaled on the right.

In Table 7.1 the responses of the wetland complex to twenty storm events from 1998 to 2005 are compiled. The events have been ranked by total heat export for unmitigated runoff from the parking lot/asphalt (Herb et al. 2006b). In all cases, the wetland basin reduces runoff temperature and heat export rate, compared to the wet detention pond. The wetland complex reduced runoff temperature by 2.6 °C, on average, compared to unmitigated runoff from the asphalt parking lot. The wetland runoff temperature is lower than the asphalt runoff temperature for 15 of the 20 storms listed, but higher for 5 of the storms. Of the twenty storms listed, the highest average runoff temperature from the wetland complex was 23.1 °C.

Table 7.1. Heat export (20°C reference temperature) and runoff temperature from a wetland complex. Rainfall events were taken from six years of climate data (1998-2000, 2003-2005) recorded at the MnROAD site. Runoff temperatures and heat export rates are given at the outlets of (1) the asphalt parking lot, (2) the wet detention pond, and (3) the wetland basin. The storms are ranked by the heat export from the parking lot.

Rank	Start Day/Time	Total Heat Export (KJ/m^2)			Average Heat Export Export Rate (W/m^2)			Duration (hours)	Total Rain (cm)	Average Dew Point (C)	Average Runoff Temp (C)		
		Asphalt	Pond	Wetland	Asphalt	Pond	Wetland				Asphalt	Pond	Wetland
1	6/24/03 18:44	887.09	647.45	-1014.19	3.25	0.14	-28.17	10.00	21.22	11.46	20.96	20.83	18.5
2	7/25/99 21:29	476.84	990.74	540.99	2.38	0.11	60.11	2.50	3.18	16.00	23.41	26.93	24.7
3	7/30/99 15:44	343.87	563.06	222.12	1.70	0.06	16.45	3.75	2.06	13.81	24.01	26.42	22.7
4	6/20/05 11:30	312.93	528.22	124.31	1.65	0.08	15.35	2.25	3.82	17.06	21.96	23.33	21.0
5	7/14/98 19:59	252.29	1134.39	503.11	1.17	0.31	25.41	5.50	5.61	13.74	21.07	24.81	22.6
6	9/19/98 15:44	225.15	117.34	-101.30	1.24	0.02	-28.14	1.00	1.47	8.54	23.79	22.10	16.9
7	6/22/99 15:14	219.33	241.46	78.92	0.97	0.03	3.81	5.75	1.46	14.19	23.23	23.58	21.4
8	7/23/05 9:00	195.00	427.18	192.87	1.02	0.06	23.81	2.25	1.92	19.72	22.44	25.37	23.1
9	8/25/04 16:44	188.08	109.29	-162.53	0.94	0.01	-15.05	3.00	2.96	15.66	21.50	20.87	18.5
10	7/13/99 22:15	139.65	218.01	101.58	0.75	0.02	18.81	1.50	0.98	20.99	23.45	25.90	23.6
11	7/2/03 23:45	126.20	616.74	296.08	0.66	0.11	41.12	2.00	2.80	18.08	21.07	25.25	22.9
12	8/19/98 19:44	124.19	192.62	60.03	0.62	0.04	5.13	3.25	1.17	15.73	22.55	24.03	21.5
13	7/25/05 15:14	120.30	180.70	-13.76	0.61	0.02	-1.18	3.25	1.10	10.91	22.73	23.86	19.8
14	9/21/05 17:30	100.30	80.88	-767.04	0.50	0.01	-65.56	3.25	5.65	7.93	20.42	20.33	16.7
15	7/7/98 16:59	95.85	66.84	24.56	0.53	0.02	6.82	1.00	0.33	17.62	28.87	25.02	21.1
16	8/12/00 8:30	92.19	65.57	16.83	0.49	0.01	3.74	1.25	0.26	17.99	27.71	26.35	22.6
17	7/11/04 3:14	86.53	412.82	178.06	0.41	0.07	9.42	5.25	2.74	18.49	20.75	23.58	21.8
18	5/15/98 15:29	81.98	43.23	-153.20	0.43	0.05	-24.32	1.75	1.65	10.17	21.17	20.64	17.1
19	8/9/05 12:44	74.91	32.64	2.98	0.42	0.00	1.10	0.75	0.21	14.56	30.22	25.77	20.9
20	7/11/03 13:15	70.12	32.86	-9.66	0.39	0.01	-2.68	1.00	0.28	15.82	27.27	23.19	19.2
	Average	210.6	335.1	6.0	1.01	0.1	3.3	3.0	3.0	14.9	23.4	23.9	20.8
	Standard Deviation	191.5	323.8	360.2	0.75	0.1	27.2	2.2	4.6	3.6	2.9	2.1	2.3

VIII. Conclusions

Two wetland basin models have been developed to simulate the ability of wetlands to mitigate temperature in heated surface runoff. In the absence of hydraulic short circuiting, the temperature mitigation capacity of a wetland basin is mainly a function of the storage volume and the degree of vegetative cover, e.g. emergent vegetation. For wetland basins with well-controlled outflow rates, hydraulic short circuiting was not found to have a major effect on thermal mitigation. It will be appropriate to collect additional field data in wetland basins to validate the model for hydraulic short circuiting.

The average outflow temperature and heat export of a wetland basin for a particular storm event is influenced by climate conditions both prior to and after the event. The temperature of the standing water in a basin available to mitigate warm inflows depends on the climate conditions for a period of several days prior to the storm event. Wetland basins with relatively long hydraulic retention times may take several days or weeks to drain the inflow from a storm event, so that the average outflow temperature can be strongly influenced by climate conditions after the storm event.

The wetland basin model was used in conjunction with a model for a wet detention pond to simulate a wetland complex. The wetland complex was found to reduce runoff temperature by, 2.6°C, on average, compared to unmitigated runoff from an asphalt parking lot. This reduction in temperature is attributable to shading from emergent vegetation. The reduction in runoff temperature, combined with the slow hydraulic responses, leads to large reductions in both the total heat export and the heat export rates. However, during very warm weather, the wetland outflow temperature did exceed 20 °C for periods of up to several days.

Acknowledgements

This study was conducted with support from the Vermillion River Watershed Joint Powers Board (VRWJPB) and the Minnesota Pollution Control Agency (MPCA) under contract with the University of Minnesota, Minneapolis, MN.

References

Andradottir, H.O., and H.M. Nepf (2000). Thermal mediation in a natural wetland: Measurements and modeling. *Water Resources Research*, 36(10): 2937-2946.

Fang, X. and H.G. Stefan (1991). Integral Jet Model for Flow From an Open Channel into a Lake or Reservoir, Project Report No. 315, St. Anthony Falls Hydraulic Laboratory, University of Minnesota, May 1991, 206 pp.

Fang, X. and H. G. Stefan (2000). Dependence of Dilution of a Plunging, Submerged Discharge Over a Sloping Bottom on Inflow and Bottom Friction" *Jour. of Hydraulic Research,* Vol. 38, No. 1, 15-26, Jan. 2000.

Hall, B.R., and G.E. Freeman, 1994. Effects of Vegetation on Hydraulic Roughness and Sedimentation in Wetlands, WRP Technical Note SD-CP-2.2, U.S. Army Corps of Engineers Waterways Experiment Station, Vicksburg, MS.

Herb, W.R, M. Weiss, O. Mohseni and H.G. Stefan (2006a). Hydrothermal Simulation of a Stormwater Detention Pond or Infiltration Basin. Project Report No. 479, St. Anthony Falls Laboratory, University of Minnesota, September 2006, 35pp.

Herb, W.R, B. Janke, O. Mohseni and H.G. Stefan (2006b). Estimation of Runoff Temperatures and Heat Export from Different Land and Water Surfaces. Project Report No. 488, St. Anthony Falls Laboratory, University of Minnesota, December 2006, 29 pp.

Herb,W.R., B.Janke, O.Mohseni and H.G.Stefan (2006c). All-weather ground temperature simulation model. Project Report 478, St. Anthony Falls Laboratory, University of Minnesota, 53pp.

Kadlec, R.O. (1994). Detention and mixing a free water wetlands. *Ecological Engineering*, 3: 345-380.

Appendix I. A model for a jet entering a basin with constant depth

The inflow to a wetland is treated as a jet, including the effects of friction and entrainment. The governing equations for the average velocity and width of a slot jet as it flows into a wide basin of constant depth are (Fang and Stefan, 1991):

(1) $$\frac{\partial}{\partial x}\left(\frac{u_m}{u_o}\right) + A_4 \frac{u_m}{u_o} + A_5 \exp(A_4 x)\left(\frac{u_m}{u_o}\right)^3 = 0$$

(2) $$\frac{b(x)}{B_o} = \frac{\exp(-A_4 x)}{2A_3}\left(\frac{u_m}{u_o}\right)^{-2}$$

where $A_4=c_f/(2H_o)$, $A_5=2\alpha_e/(A_oB_o)$, B_o is the width of the jet inlet, A_o=1.4142, A_3=0.37639, u_o is the mean velocity at the inlet, u_m and b(x) are the mean jet velocity and width, respectively, as a function of streamwise distance from the inlet, x, and α_e is the rate of entrainment. Fang and Stefan assume a constant entrainment rate, $\alpha_e = 0.4$, which leads to an exponential increase in the width of the jet. In a similar model for jets between parallel plates, Chu and Baines (1989) assumed a constant rate of increase in jet width based on experimental data, which leads to a rate of entrainment that decreases to zero with distance. There is insufficient data for the high wall friction environment of wetlands to evaluate which assumption is better. Closed form solutions can be obtained for Equations 1 and 2 using the assumption of constant entrainment rate, so that this assumption was tentatively chosen for this study.

Fang and Stefan utilized numerical solutions of Equation 1 to show the solution behavior, however, a closed-form solution of Equation can be obtained as:

(3) $$\frac{u_m(x)}{u_o} = \left[(1+A_6)\exp(2A_4x) - A_6\exp(2A_4x)\right]^{-1/2}$$

where $A_6 = 2A_5/A_4$. The corresponding functions for the jet width, b(x), and flow rate, Q(x) are:

(4) $$\frac{b(x)}{B_o} = \frac{\left[(1+A_6)\exp(A_4x) - A_6\right]}{2A_3}$$

(5) $$\frac{Q(x)}{Q_o} = \frac{u_m(x)}{u_o}\frac{b(x)}{B_o}$$

By integrating Equation 3 over distance, an equation estimating the time t_L for the jet to traverse a distance L can be obtained:

(6) $$t_L = \frac{A_5 L^2}{U_o\left(\sqrt{1+A_6(1-\exp(-A_4L)} - 1\right)}$$

A dimensionless time parameter, t*, can be defined that normalizes t_L to the velocity and length scales, U_o and L:

$$(7)\quad t^* = \frac{t_L U_o}{L} = \frac{A_5 L}{\sqrt{1 + A_6 (1 - \exp(-A_4 L)} - 1}$$

For example, if t*=2, then the jet with entrainment and friction effects takes 2x longer to traverse a length L. Finally, by setting the normalized jet velocity u_m/U_o equal to a constant ratio, r_u, less than unity an estimate for the length of the jet can be obtained:

$$(8)\quad L_j = \frac{1}{A_4} \mathrm{Ln}\left(\frac{A_6 + \sqrt{A_6^{\,2} + 4(1 + A_6)/r_u^{\,2}}}{2(1 + A_6)} \right)$$

Figures A.1 to A.5 plot several results of the analytic model for jet length, width, velocity, and flow rate for a range of parameter values.

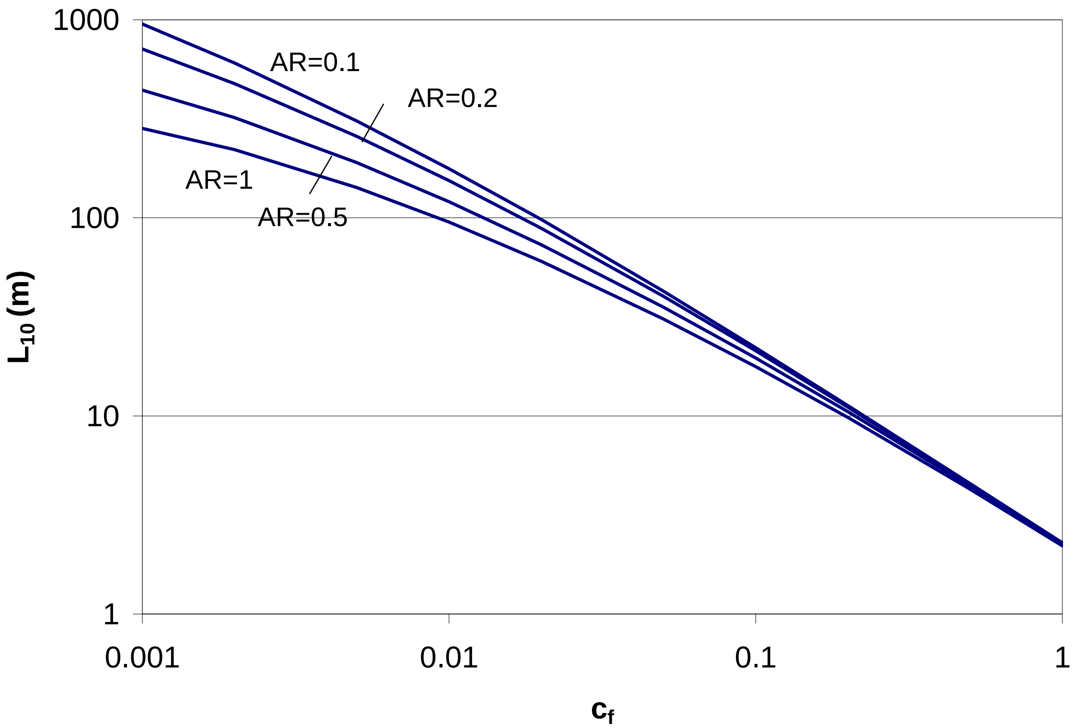

Figure A1. Characteristic jet length (L_{10}) vs. friction coefficient (c_f) for several jet aspect ratios (AR=H_o/B_o). L_{10} is the distance at which the jet velocity decreases to 10% of its inlet value.

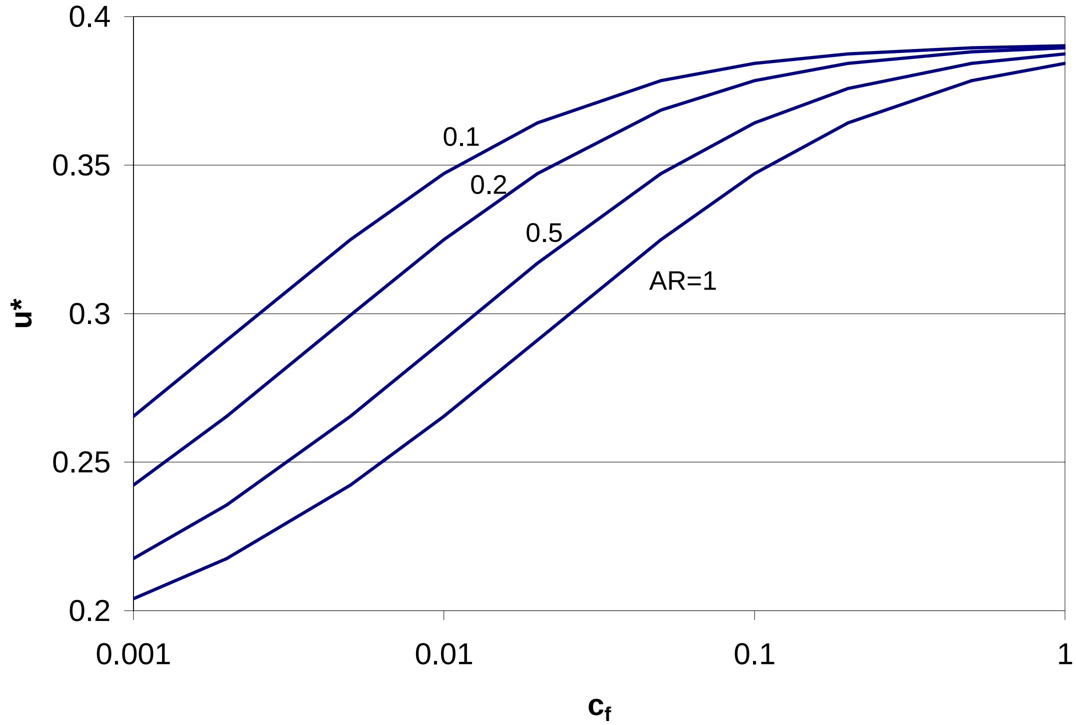

Figure A2. Characteristic average jet velocity (u*) vs. friction coefficient (c_f) for several jet aspect ratios ($AR=H_o/B_o$). u* is the ratio of the average velocity to the inlet velocity over the length t_L..

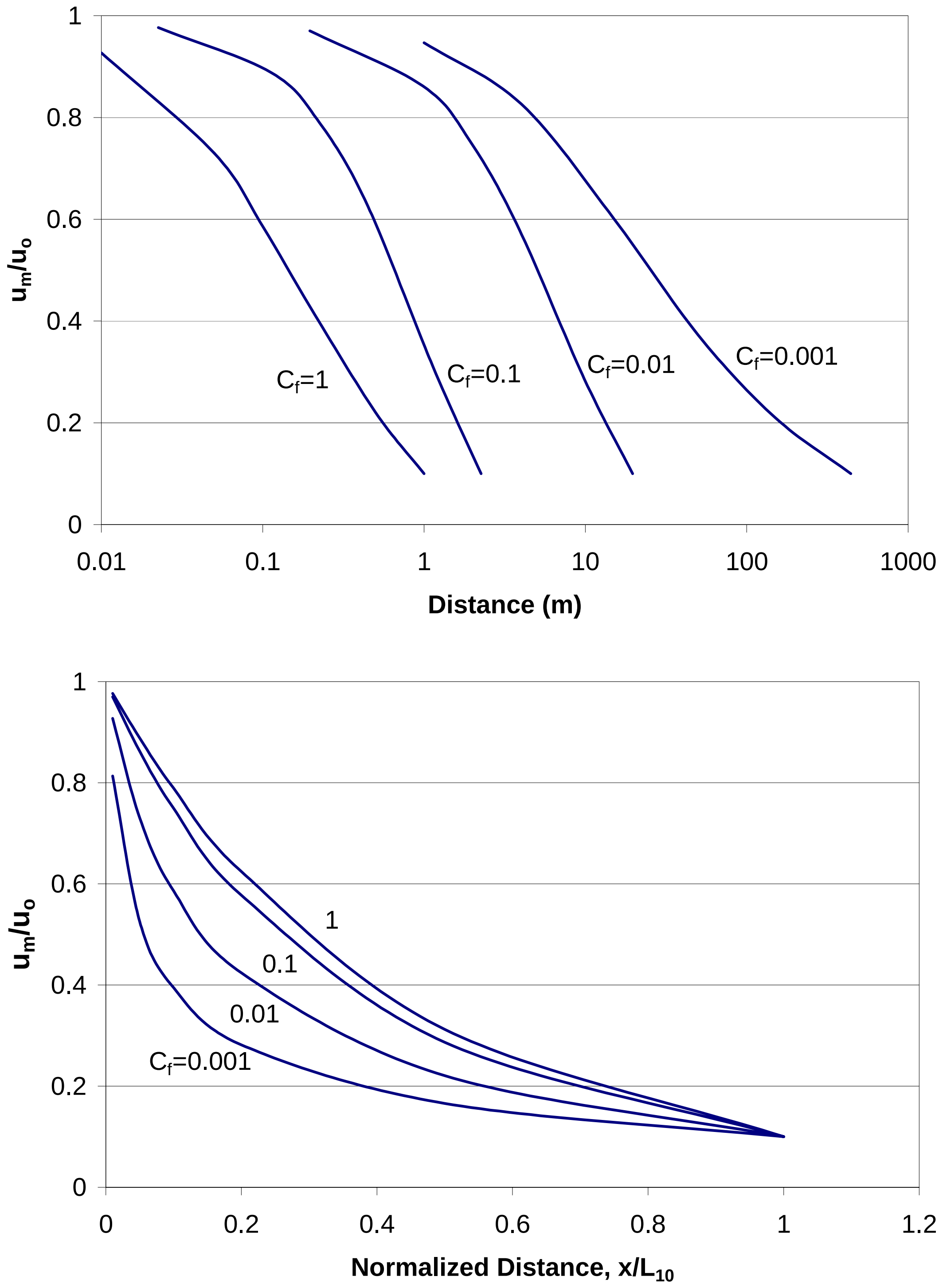

Figure A3. Normalized velocity vs. distance (upper panel) and normalized distance (lower panel) for varying friction coefficients C_f and $H_o = B_o/2$.

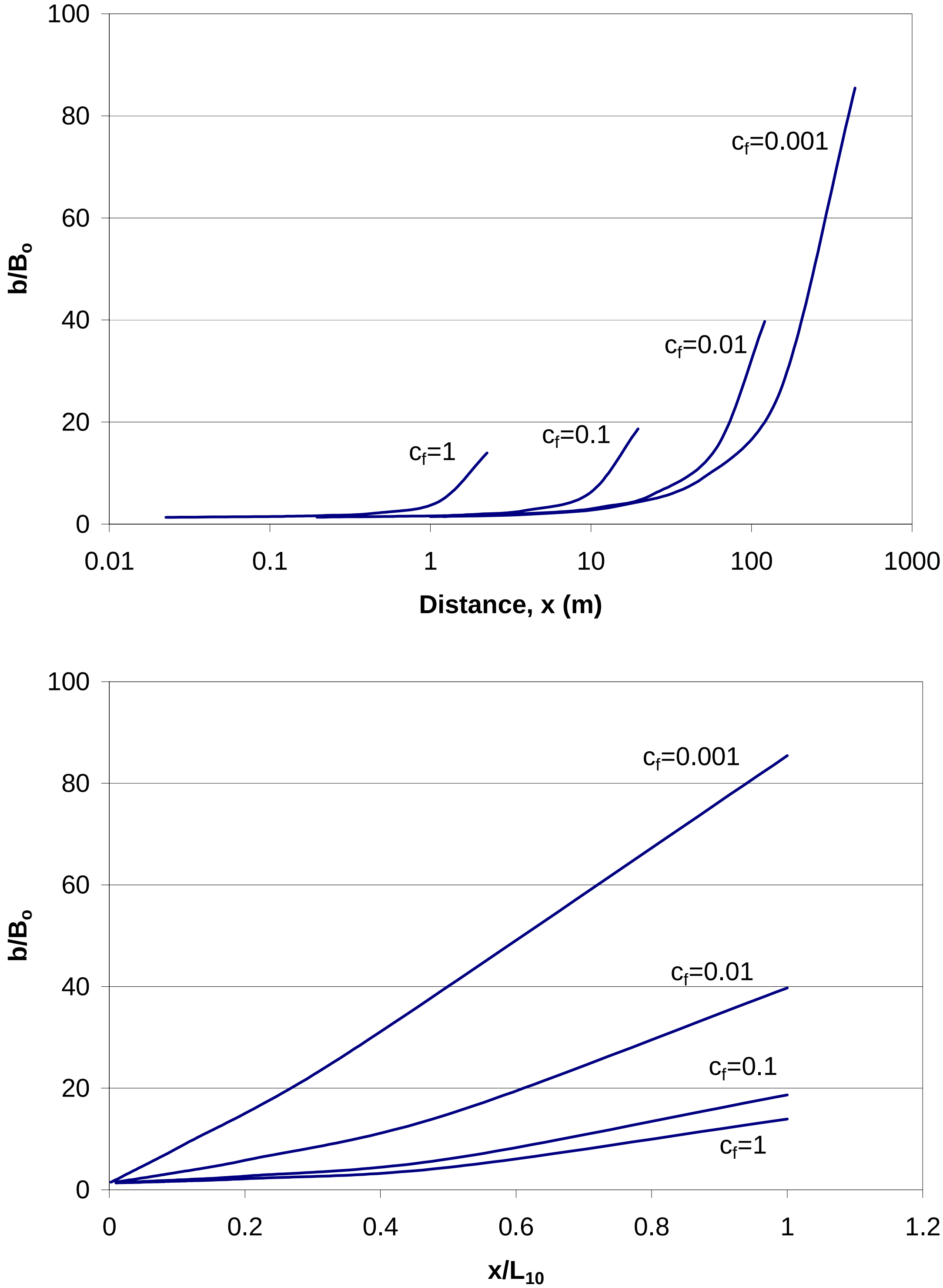

Figure A4. Normalized jet width vs. distance (upper panel) and normalized distance (lower panel) for several friction coefficients c_f and $H_o = B_o/2$.

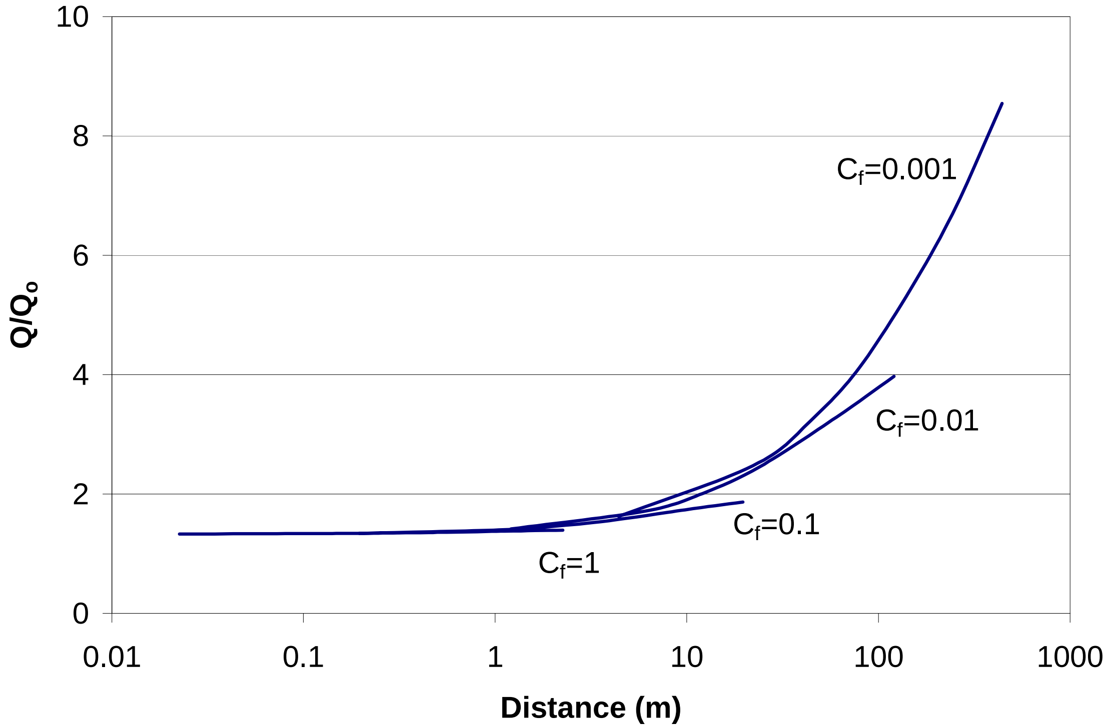

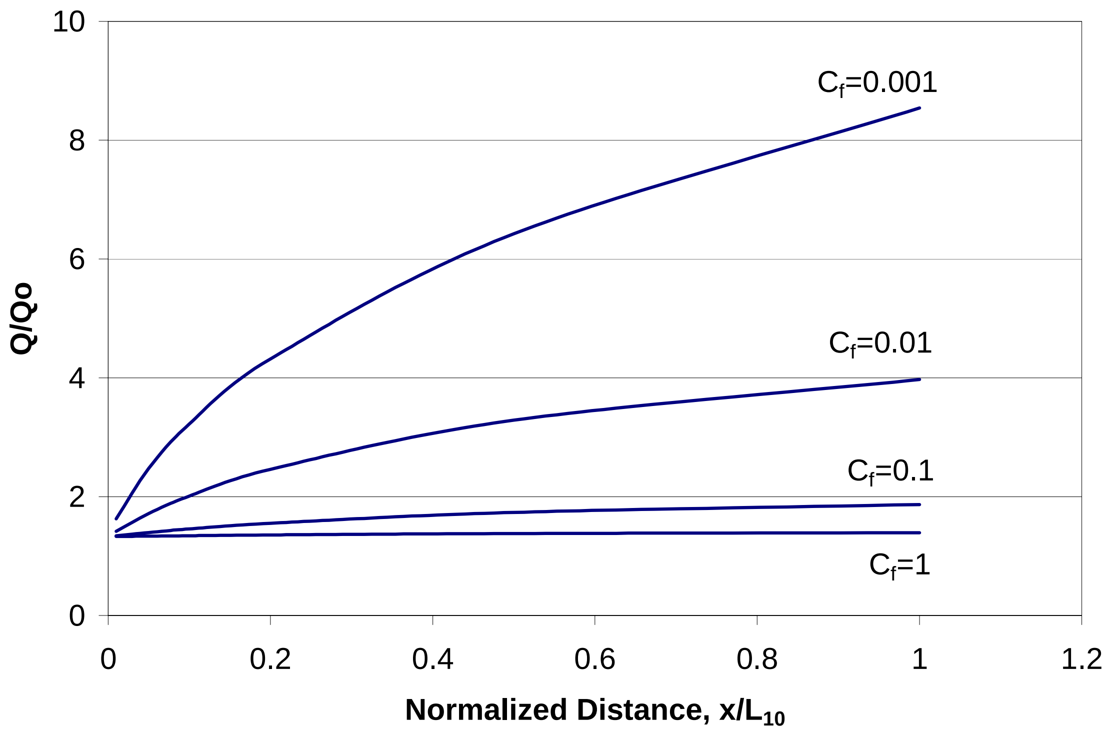

Figure A5. Normalized jet width vs. normalized distance for several friction coefficients C_f and $H_o = B_o/2$.